HERCULES-2 Project

Fuel Flexible, Near Zero Emissions, Adaptive Performance Marine Engine

Deliverable: 7.6

Experimental assessment of SCR reduction agent injection systems with sensors for feedback control

Revision Final

Nature of the Deliverable:	Demonstrator
Due date of the Deliverable:	1.3.2018
Actual Submission Date:	5.3.2018
Dissemination Level:	Public

Contributors:	Wärtsilä Finland Wärtsilä Spain
Work Package Leader Responsible:	Jukka Leinonen (Wärtsilä Finland)

Start date of Project: 01/05/2015 Duration: 42 months

Grant Agreement No: **634135-HERCULES-2**

HORIZON 2020
The EU Framework Programme for Research and Innovation

TABLE OF CONTENTS

Executive Summary

Reducing agent injection has a critical role in the reliability, efficiency and operation costs of the SCR system. By understanding the ammonia mixing behaviour and chemical reactions on the catalyst surface, a sensor based feedback could be used to maximizing the SCR performance and minimizing the reducing agent consumption. In this study, 1D- and CFD-simulations were utilized to understand and optimize the urea mixing before the SCR, and to enable further development of such SCR sensor feedback based controls under varying conditions. Simulations and actual demonstration measurements on 4-stroke marine engine equipped with SCR showed that the reduction agent reactions and eventually emission performance are affected by the mixing of the ammonia, SCR catalyst temperature and the adsorption of the ammonia on the catalyst surface.

Valuable information about the temperature behaviour was achieved with simple NOx sensor, while the ammonia sensor planned to be used in these studies could not survive the conditions of residual fuel operation.

1 Introduction

In marine engines, the SCR performance is typically verified in certification, and the installations in the field are operated with a pre-set reducing agent injection rates determined by the engine emissions and designed NOx reduction needs. This approach has proven to be robust and functional for rough marine conditions. However, different operating conditions and engine operating profiles affect the engine emissions, and by further development of the measurement and control systems, an improved emission performance could be achieved. By understanding the ammonia mixing behaviour and chemical reactions on the catalyst surface, a sensor based feedback could be used to maximizing the SCR performance and minimizing the reducing agent consumption.

2 Objectives

Objective of this work was to improve SCR reducing agent injection, find solutions for sensor based feedback control, and evaluate feasibility of the sensors under marine engine exhaust conditions.

3 Tools and testing arrangement

CFD simulations for exhaust flow distribution and ammonia distribution were carried out with STAR CCM+ V. 11.06. For simulating the effect of temperature on ammonia absorption GT-power was used. After simulation, emission measurements on full scale SCR installation on medium speed 4-stroke engine were carried out.

4 Results

4.1 *Urea mixing and screening of improved mixing arrangements*

Two different model geometries were considered for CFD-simulation: An SCR model which was used for the validation of the simulation, and a straight pipe configuration where different mixer designs were investigated. All models included exhaust pipe from the engine, reductant agent injector, static mixer, SCR reactor and the piping downstream of the reactor. The catalyst layers were simulated as a porous region and the rest of the parts were defined as fluid regions.

The working fluids in the system are the exhaust gas flow coming from the engine and the reductant injection. For the exhaust gas inlet a constant mass flow with uniform composition and velocity profile was used, and for the outlet a constant pressure outlet condition. All walls were assumed to have adiabatic and no-slip boundary conditions.

4.1.1 Urea water solution (UWS) Decomposition models

In the chemical reaction approach, urea decomposes very fast into equal amounts of isocyanic acid (HNCO) and ammonia (NH_3). Figure 1 shows the transport of HNCO and NH_3 at a mid-plane section of the pipe. It can be seen that the transport of NH_3 and HNCO is identical.

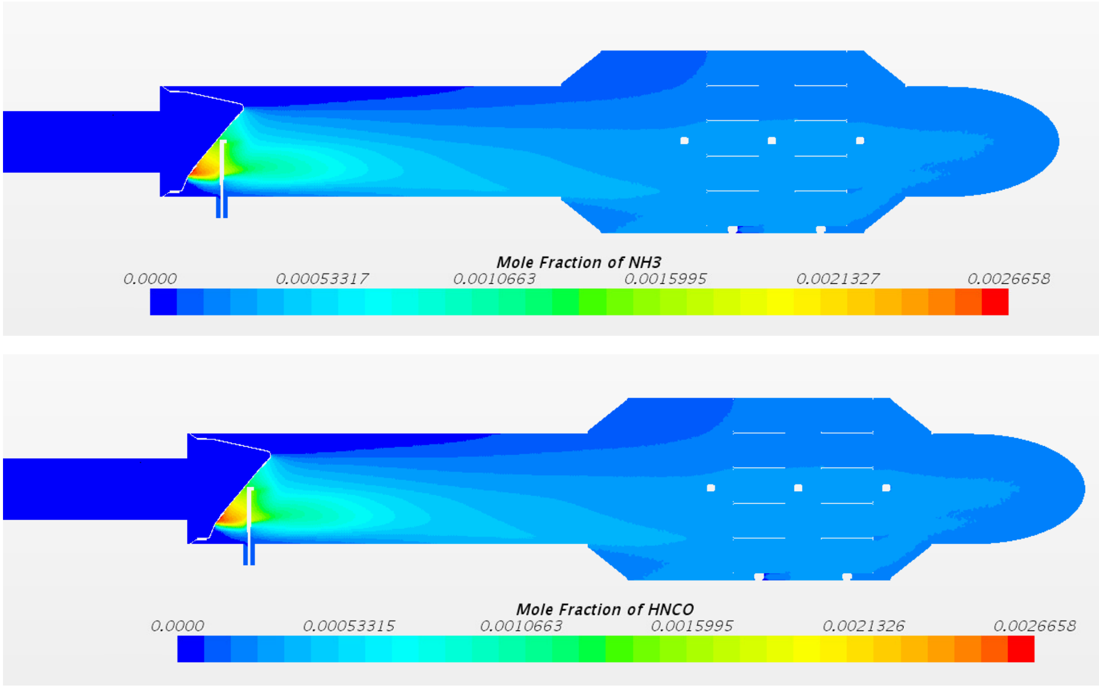

Figure 1. Transport of ammonia and isocyanic acid with evaporation approach.

The evaporation approach assumes that all urea evaporates to NH_3. Figure 2 shows the transport of NH_3 at a mid-plane section of the pipe for chemical reaction approach, and it follows the same trend as for the HNCO and NH_3 transport.

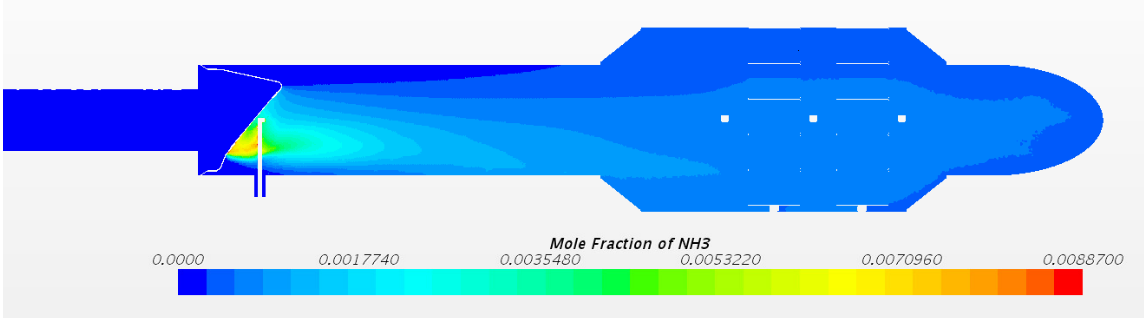

Figure 2. Transport of ammonia with chemical reaction approach.

Figure 3 shows comparison of NH_3 UI for evaporation and chemical reaction approach at the surface into the reactor, and first and second catalyst layers. The Figure shows that there is no significant difference between the two approaches when it comes to uniformity of NH_3.

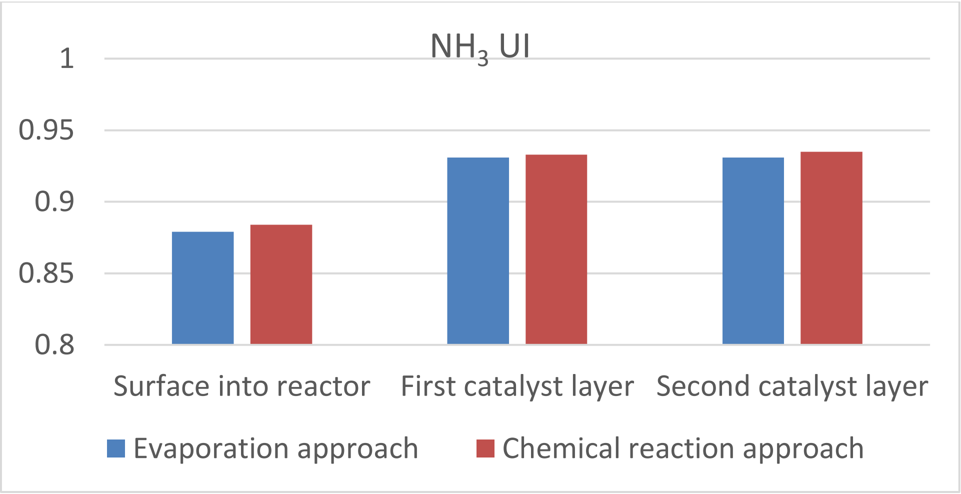

Figure 3. Comparison of ammonia UI for evaporation and chemical reaction approach at surface into the reactor and at the catalyst surfaces.

4.1.2 UWS injection for 25 % and 100% load

In Figure 4 the UI of velocity and NH_3 along the mixing pipe for 25 and 100 % load are presented. The velocity uniformity is the same for both loads and reaches its maximum value already after 2.5 m. An interesting finding is that the uniformity of NH_3 is higher for 25 % load. Already after 0.5 m the UI of NH_3 for 25% load is 10% higher compared to 100 % load condition. Along the mixing pipe the difference decreases and at the catalyst surface the difference is only 3 %.

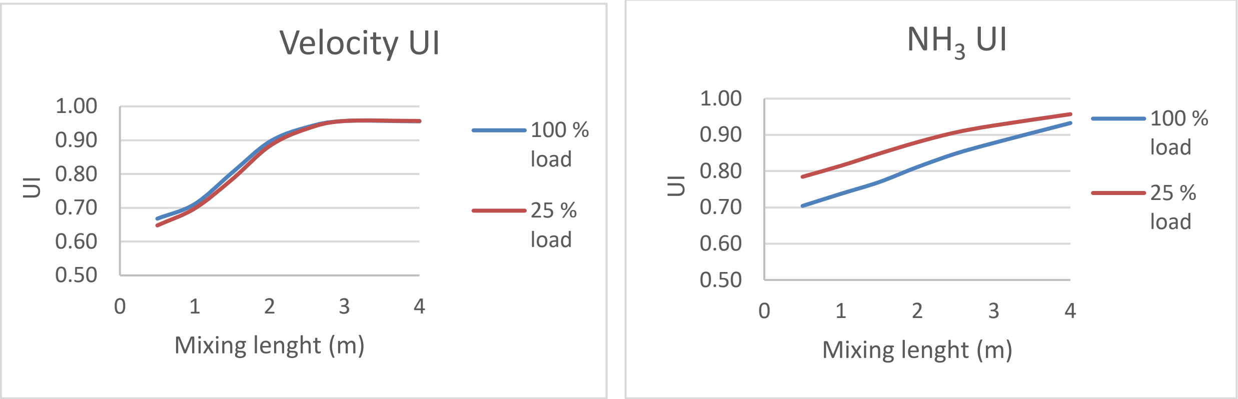

Figure 4. UI index of velocity and ammonia plotted as a function of the mixing length for 25 and 100 % load.

4.1.3 Mixing design

Figure 5 presents the three different mixer geometries considered. The first one is a plate mixer, which is used as a reference case in this study. The second one is a High Efficiency Vortab (HEV) mixer. Three different configurations of the HEV mixer were studied. Two of the HEV configurations have different lengths of the tabs and the third has the second layer of tabs rotated 45° with respect to the first circular tabs. The third mixer geometry is a swirl mixer with 8 blades. The blade mixer was simulated with two different blade size variations.

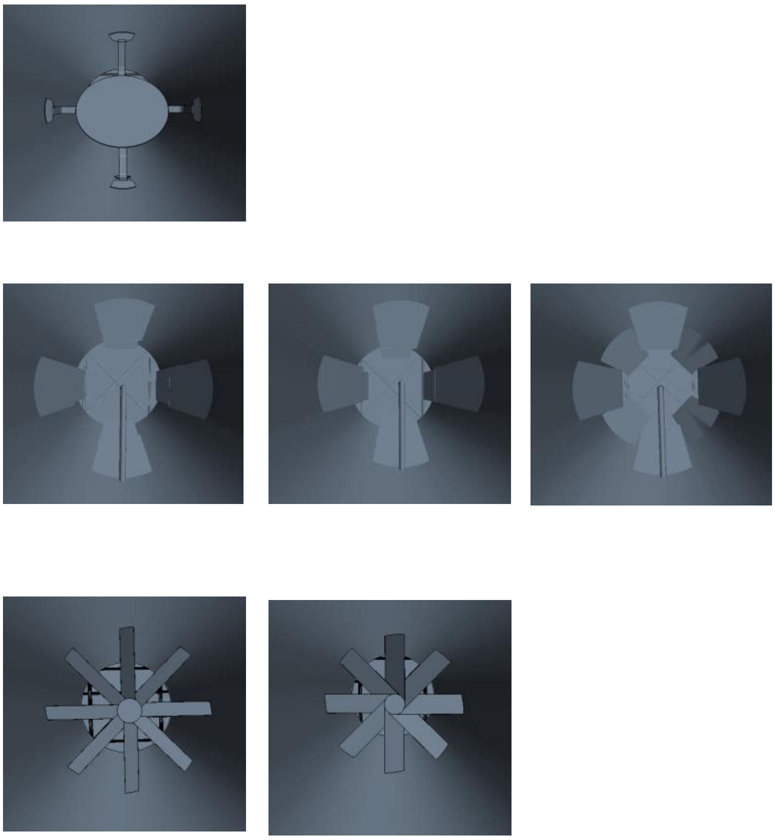

Figure 5. Mixer geometries: Plate mixer, HEV mixer & blade mixer.

The mixer geometries were analysed by comparing the velocity UI and NH_3 UI as a function of the mixing length in Figures 6-9. Ammonia gas was simulated as a reference to see if the water evaporation from the UWS droplets makes the mixing much slower. NH_3 gas was introduced as single point injection from the same location as the UWS solution. The plate mixer is used as a reference case to compare the result, since it is used in many SCR applications.

4.1.3.1 HEV Mixer

Looking at the velocity UI along the mixing pipe in Figure 6, a high uniformity is observed over the pipe length. The lowest uniformity is after the second tab and after that the uniformity starts to increase and reaches its maximum value at 3 m.

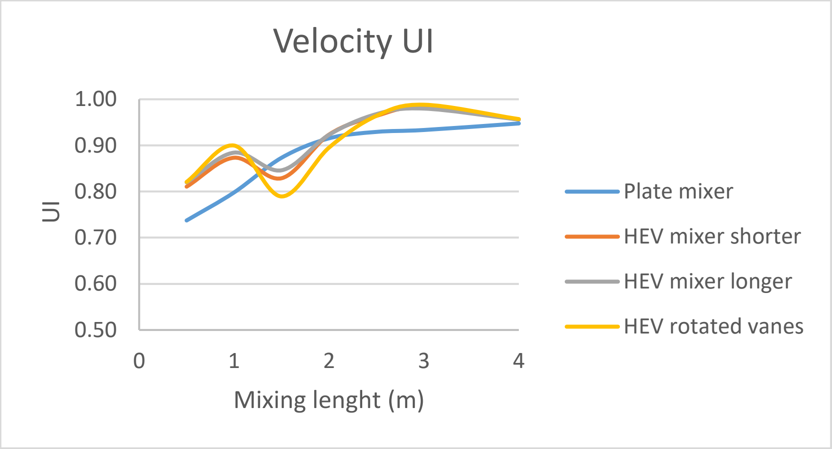

Figure 6. UI index of velocity plotted as a function of the mixing length for HEV mixer configurations.

Figure 7 compares the UI of NH_3 along the mixing pipe for both NH_3 gas injection and UWS injection. The plate mixer has 60 % higher UI already after 0.5 m compared to the HEV mixers. With NH_3 gas injection the plate mixer and the HEV mixer with longer blades have the same UI at the catalyst surface. When the reductant is injected in gas form the uniformity increase much faster compared to when UWS is injected. With UWS injection the lines are still increasing linearly at the catalyst surface which indicates that the HEV mixer requires longer mixing length to get more uniform distribution. For all HEV mixer the concentration of NH_3 is highly concentrated in the center of the mixing pipe.

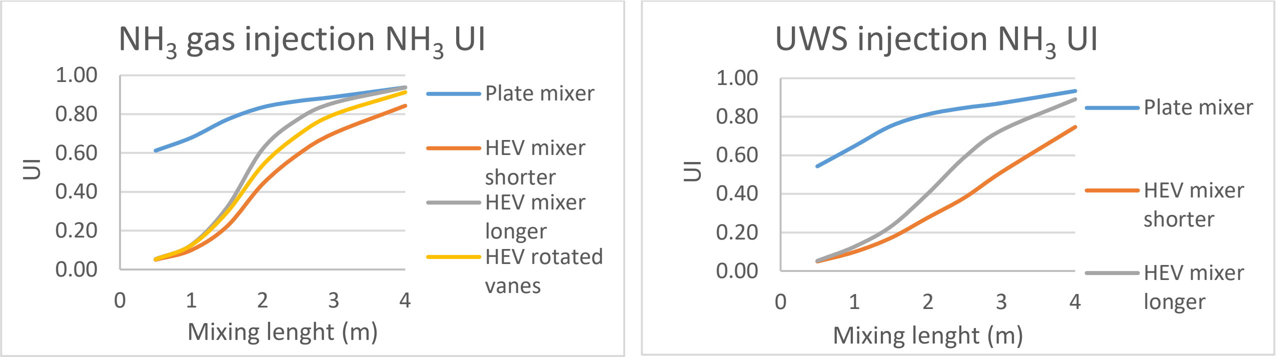

Figure 7. UI index of ammonia plotted as a function of the mixing length for HEV mixer configurations, with ammonia gas injection and UWS injection.

4.1.3.2 Blade mixer

Figure 8 represents the velocity UI along the mixing pipe for the blade mixers. High velocity uniformity along the mixing pipe is observed for both blade configurations, but a drop in the uniformity is observed after 2.5 m for the mixer with wider blades.

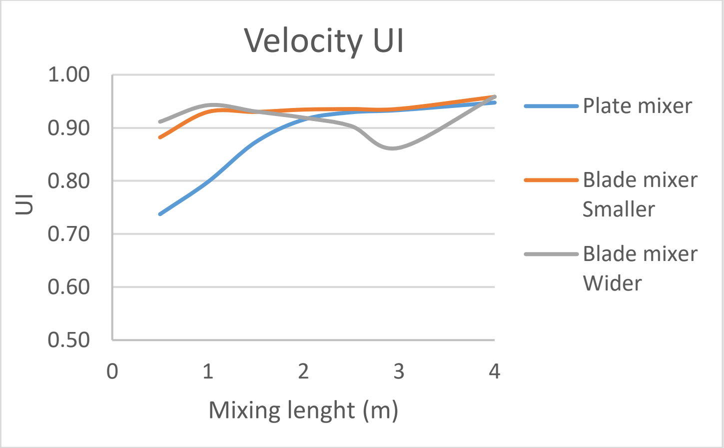

Figure 8. UI index of velocity plotted as a function of the mixing length for blade mixer configurations.

Figure 9 compares the UI of NH_3 along the mixing pipe for both NH_3 gas injection and UWS injection. No significant difference between the two reductant agent’s methods can be observed. The uniformity increases linearly, but after 3 m the UI increase more rapidly. The plate mixer has 21% higher UI after 0.5m compared to the blade mixer, but at the catalyst surface the blade mixer with wider blades have similar UI as for the plate mixer. Of the two blade mixer configurations, the blade mixer with wider blades shows the highest UI. The maximum difference of the NH_3 uniformity is at the catalyst surface, where the difference is 14 %. The transport of NH_3 along the mixing pipe is similar as for HEV mixer with a high concentration in the centre of the mixing pipe.

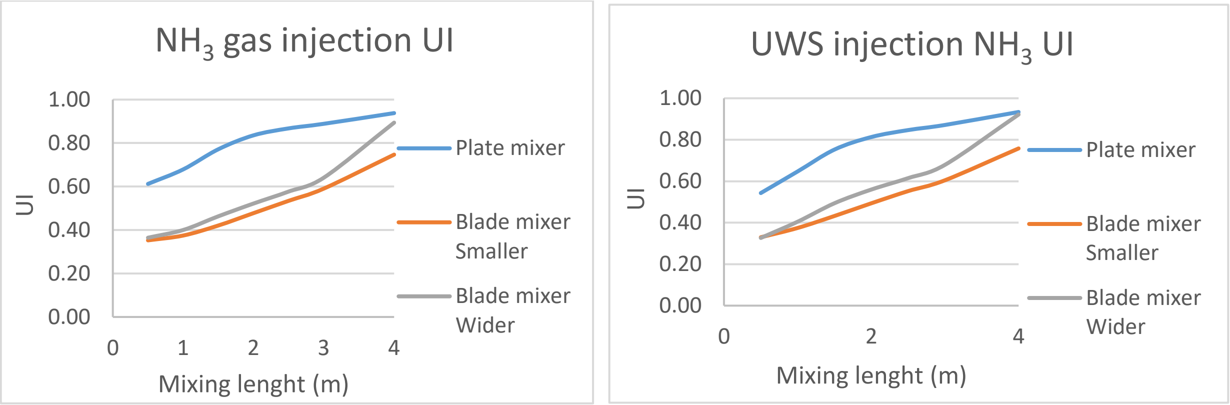

Figure 9. UI index of ammonia plotted as a function of the mixing length for blade mixer configurations, with ammonia gas injection and UWS injection.

In different mixer arrangements the pressure drop is the cost one must pay for efficient mixing. Therefore, a plot of pressure drop vs. UI of NH_3 offers an intuitive way to tell different cases apart; ideally a UI index of 1 with a minimal pressure drop would be optimum. Figure 10 summarize the results of NH_3 uniformity at the catalyst surface and pressure drop over the static mixer for both UWS injection and NH_3 gas injection.

Plate mixer has a low pressure drop and high uniformity for both reductant injection methods. HEV mixer has lower uniformity when UWS is used as a reductant, and with longer tabs the uniformity and pressure drop increases. HEV mixer with rotated tabs has the highest pressure drop, but lower uniformity compared to HEV mixer with longer tabs. The blade mixer also has similar uniformity for both injection methods. In pressure drop and NH_3 uniformity increases with wider blades.

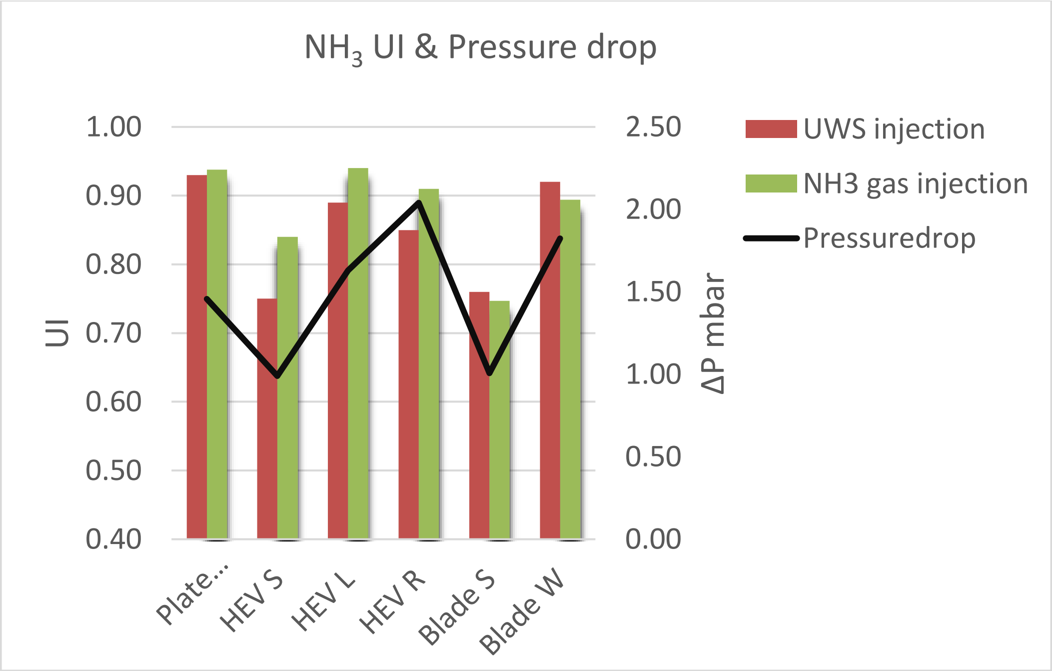

Figure 10. Comparison of pressure drop vs. ammonia uniformity at catalyst surface for urea water solution injection and ammonia gas injection.

4.2 GT-power simulation for adsorption and desorption behaviour for feedback control

To simulate the adsorption and desorption behaviour of the SCR catalyst, also a GT-power model was created. This behaviour is one of the important parameters in a feedback based control to both limit NH_3 slip and maximize NO_x conversion. Most of the stand-alone example and models in GT-Power are set up to run experiments from a synthetic gas bench. Such experiments are designed to show a certain effect like adsorption or NOx reduction by the “fast” SCR reaction. In these simulations, 8-step mechanism model was used in the simulations. The reactions consist of detailed reaction mechanism for Standard and Fast SCR:

1) $V + NH_3 => VNH_3$ (Adsorption of NH_3)
2) $VNH_3 => V + NH_3$ (Desorption of NH_3)
3) $VNH_3 + 0.75O_2 => 0.5N_2 + 1.5H_2O + V$ (NH_3 oxidation)
4) $NO + VNH_3 + 0.25O_2 => N_2 + 1.5H_2O + V$ (Standard SCR)
5) $NO + VHNO_3 + VNH_3 => N_2 + 2H_2O + NO_2 + 2V$ (Fast SCR)
6) $2NO_2 + VNH_3 => N_2 + H_2O + VHNO_3$ (Nitrat formation)
7) $VNH_3 + 0.75NO_2 => 0.875N_2 + 1.5H_2O + V$ (NO_2 SCR)
8) $VNH_3 + VHNO_3 => N_2O + 2H_2O + 2V$ (N_2O Formation)

4.2.1 Effect of temperature

TPD (Temperature programmed desorption) model shows how the stabilization of ammonia adsorption takes significantly longer time at lower temperatures, and also the amount of ammonia released by the fast temperature ramp is much higher. Figure 11 shows simulations where NH_3 is fed into the catalyst with a constant mass flow and inlet gas temperature until outlet concentration is equivalent to inlet concentrations (steady state). After steady state has been reached NH_3 feed is shut off. After the outlet NH_3 concentration is close to zero the temperature of the exhaust gas is increased at a linear rate up to 500°C and desorption of the ammonia from the catalyst modelled.

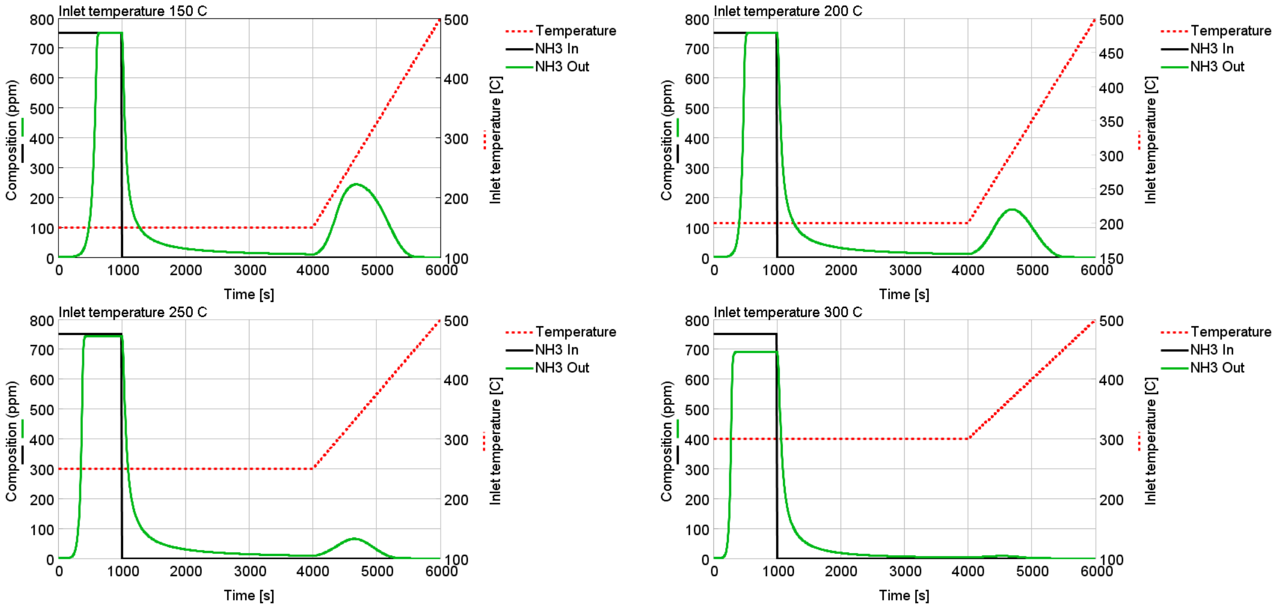

Figure 11. The figure shows the progress of the NH_3 outlet concentration upon opening and shutting down the NH_3 feed at four different adsorption temperatures, followed by a linear temperature increase at 4000 s.

When increasing the temperature, shorter adsorption times are observed before the ammonia starts to break through (respectively ≈ 50, 45, 40 and 30 s for temperatures= 150, 200, 250 and 300 ◦C). The amount of NH_3 adsorbed onto the catalyst surface is reduced, which is seen also during the temperature increase at 4000 s. In all figures the desorption of ammonia is complete at around 430°C.This also confirms that the SCR have lower adsorption capacity at higher temperatures. Decreased ammonia storage capacity caused by higher temperature can also cause ammonia slip pulses during rapid increase in temperature.

Effect of temperature is also expressed in Figure 12. In this simulation, constant NOx and ammonia flow concentrations are introduced to SCR inlet at 0 second, and simulation result is expressed after the catalyst layers. At low temperatures (200-250°C) the adsorption of the ammonia is slow and catalytic activity too low to consume all ammonia for the NOx reduction. At higher temperatures only small amount of ammonia is adsorbed on the catalyst surface, leaving more ammonia available for the NOx reduction and the stabilization is faster. Higher temperature increases the catalytic activity and no ammonia slip is observed.

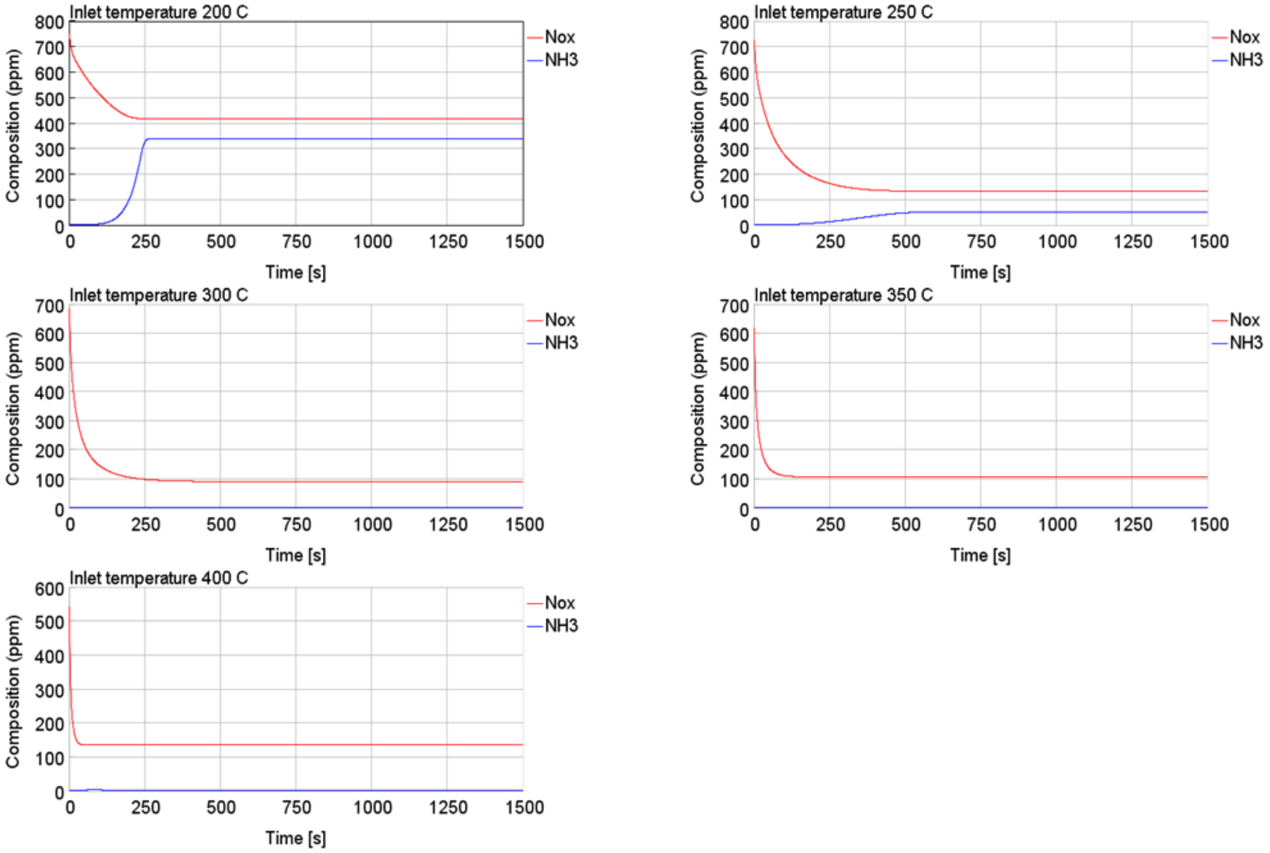

Figure 12. Simulation of NOx and ammonia concentrations after the catalyst at different temperatures.

4.3 Demonstration and studies for feedback control

4.3.1 Measurement setup

To demonstrate the principle of feedback control and to verify simulated results of urea mixing behaviour and flow distribution, emissions measurements of 4-stroke engine equipped with SCR were carried out. Measurements were carried out with FTIR equipment. NH_3 and NOx concentrations were measured after the first catalyst layer from 9 different probe points spread out on the surface area of the catalyst as illustrated in Figure 12. Measurements were done for 100 % and 25 % load.

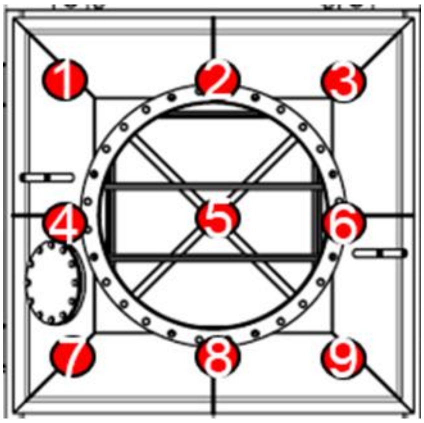

Figure 13. Location of measurements points downstream of the first catalyst layer.

4.3.2 Comparison of CFD result and the measured results

Simulated NH_3 and NO_x concentration for the 9 probe points are compared with the measured values in Figures 14-16. In our earlier studies on SCR simulation (for example reported in Hercules C), we have compared the flow distribution and ammonia mixing concentrations with the measured results. In this simulation, the approach was taken one step forward by combining the flow distribution and ammonia concentrations with the chemical reaction model for the NOx reduction in the catalyst. Highest concentrations of NH_3 were simulated at the middle of the catalyst face area (close to measurement points 5 and 6) and the lowest concentration at the top, close to measurement point 2. The highest velocities at the catalyst surface were simulated at higher mid-section between the measurement points 2 and 5. Higher concentration of NH_3 should increase the NOx conversion, and higher velocities should give shorter residence time for catalytic reduction and correspondingly highest NO_x and NH_3 slip after the elements.

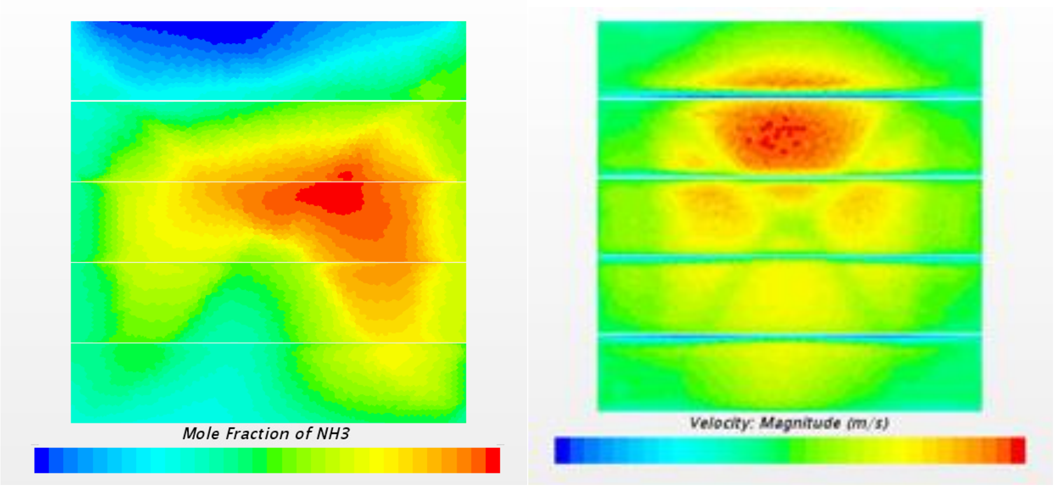

Figure 14. Simulated ammonia distribution and flow velocity at the first catalyst layer.

The difference between the simulated and measured values at full engine load are presented in Figure 15. In general, the absolute values are quite close to each other and variation in different probe points quite small. The simulated distribution indicates lowest NOx values in the mid-section of the reactor at measurement points 4-6, due to the high ammonia concentration at the same area. However, in the measured results, NOx and NH_3 levels are more stable and no significant differences are observed between the probe points.

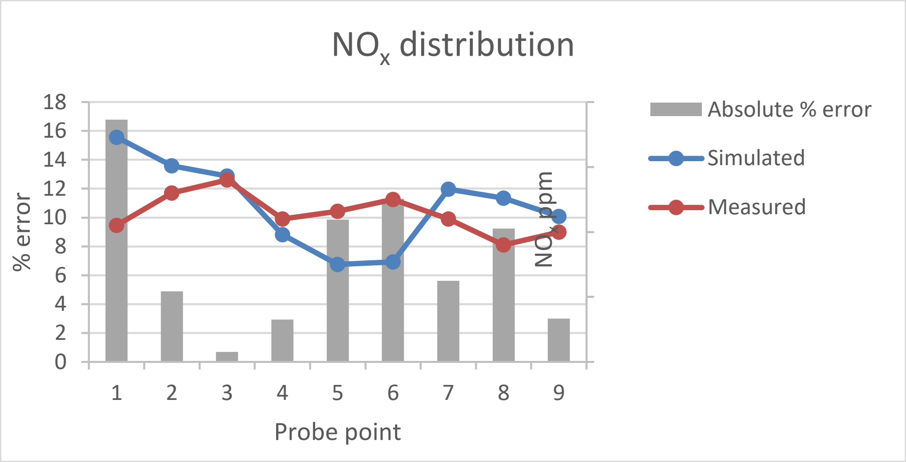

Figure 15. Comparison between simulated and measured NOx concentrations.

4.3.3 Ammonia adsorption and desorption, feedback control

Ammonia storage behaviour was studied also in real exhaust conditions with the SCR and NOx sensors. The original plan was to apply the ammonia sensor (reported in D7.2) for feedback control for minimizing the ammonia slip and optimizing the SCR response to changing conditions. Unfortunately, the sensor could not survive the conditions of residual fuel operation, and only the NOx sensors were used for the follow-up. Figure 16 shows the correlation of the ammonia sensor with FTIR when operating with ULSD fuel in the beginning of the testing. Measurements were done at different engine loads and emission concentrations. At very low values (0-3 ppm) the sensor had some background noise, but in the range of 5 to 20 ppm the readings were in good correlation with FTIR.

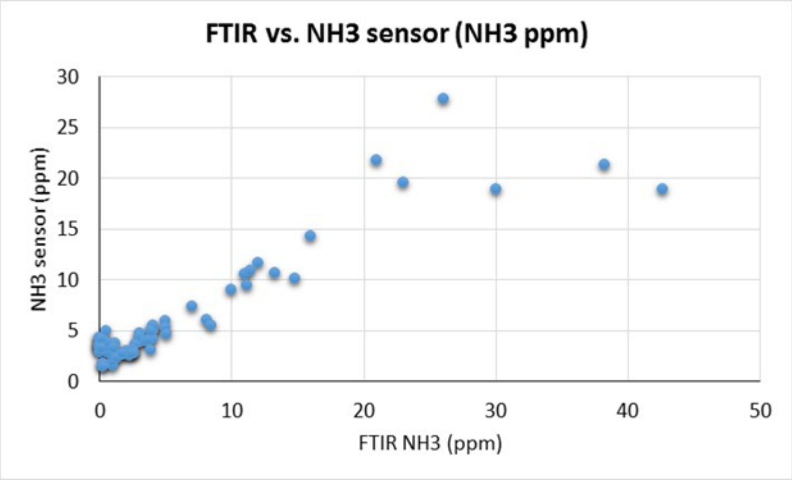

Figure 16. Correlation of ammonia sensor and FTIR in ammonia concentration measurement.

The effect of temperature on the adsorption of the ammonia (simulated in Figures 11-12) on the catalyst surface was studied with the SCR and NOx trend is presented in Figure 17. When the urea injection is started (left side of the graphs), it takes several minutes for the NOx concentration after the SCR to even out, as the NOx reduction reactions and adsorption of the ammonia on the surface stabilizes. Time required for the stabilization is seen also when the urea injection is shutdown: There is slight decrease first in the NOx emissions due to purge behaviour of the injection nozzle (urea is purged by pressurized air from the piping), after which the NOx concentration is slowly increasing to level of engine emission. When the engine exhaust temperature is increased by 30°C (right side figure), both stabilization times are shorter and indicating a lower buffering by the adsorbed ammonia.

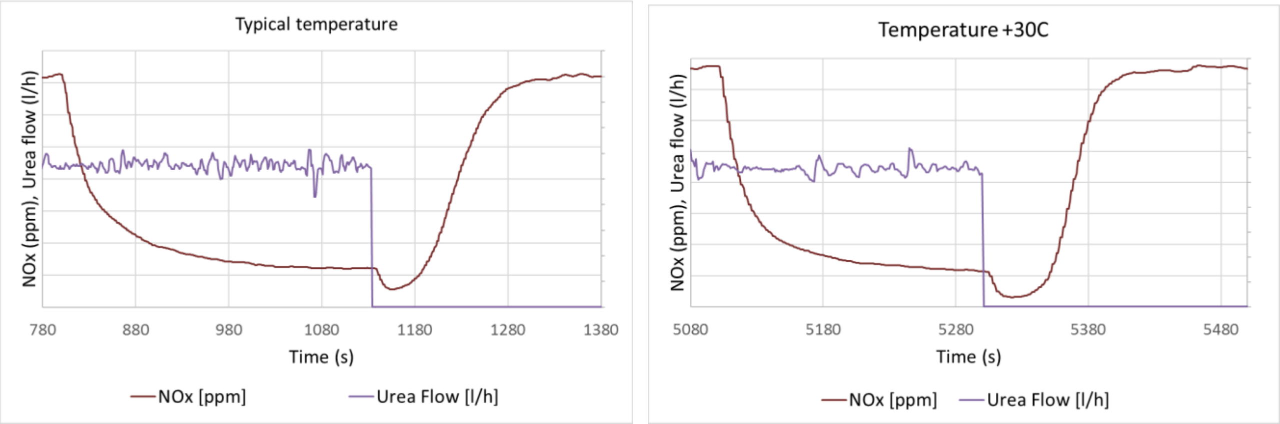

Figure 17. Effect of Exhaust temperature on adsorption and desorption of ammonia.

The buffering behaviour of the catalyst can also be seen in transient operation of the engine. In Figure 18 the engine is fast loaded from 10% to 100% load and back to 10%, and the urea is fed with pre-set flow rates. Full load conditions determine the SCR maximum performance, and therefore NOx concentration is higher, while at lower loads very low emission values are achieved (low exhaust mass flow gives long residence time for the catalytic reactions). During the loading, the ammonia adsorbed ammonia can buffer the increasing NOx mass flow, and no significant peaks are observed during the loading. In de-loading the NOx flow decreases fast while the slight delay in urea injection causes NOx value to decrease above the original level for few minutes. With optimized feedback control this should be possible to stabilize faster.

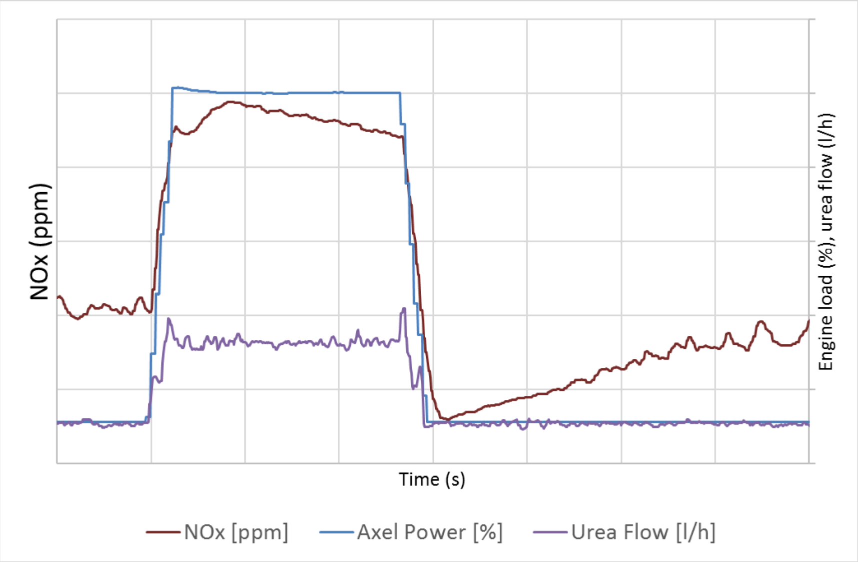

Figure 18. NOx emissions in fast loading and de-loading of the engine.

Above results show that already NOx sensors can give valuable information for controlling the reducing agent injection. However, the reactions on the surface of the catalyst are affected by NOx and NH_3 concentrations, temperatures and flow rates, and optimizing this complex equation requires lots of further testing and validation. In addition, a fast sensor for analysing the ammonia slip would enable more accurate control when operating on the maximum limits of the SCR performance and in fast transients.

5 Conclusions

For the effective use of feedback control, fast and reliable sensors are needed. In addition to flow control equipment, the catalyst behaviour under different temperatures and different NOx and ammonia concentrations needs to be understood. Developed SCR models for 1D- and CFD-simulations gave good indication of SCR performance and behaviour, and experimental tests verified similar observations. The situation is even more challenging under transient conditions, when the exhaust volume, temperature and concentrations are changing, and depending on controls the NOx emissions after the SCR will be affected. Based on the current results, it seems that there is still work to do on the development of feedback sensors for the exhaust conditions of marine fuels, and also understanding and fine-tuning the controls in real operation conditions.

6 Appendices: demonstration measurement pictures

Figure 18 View inside the SC reactor showing the rectangular catalyst bricks

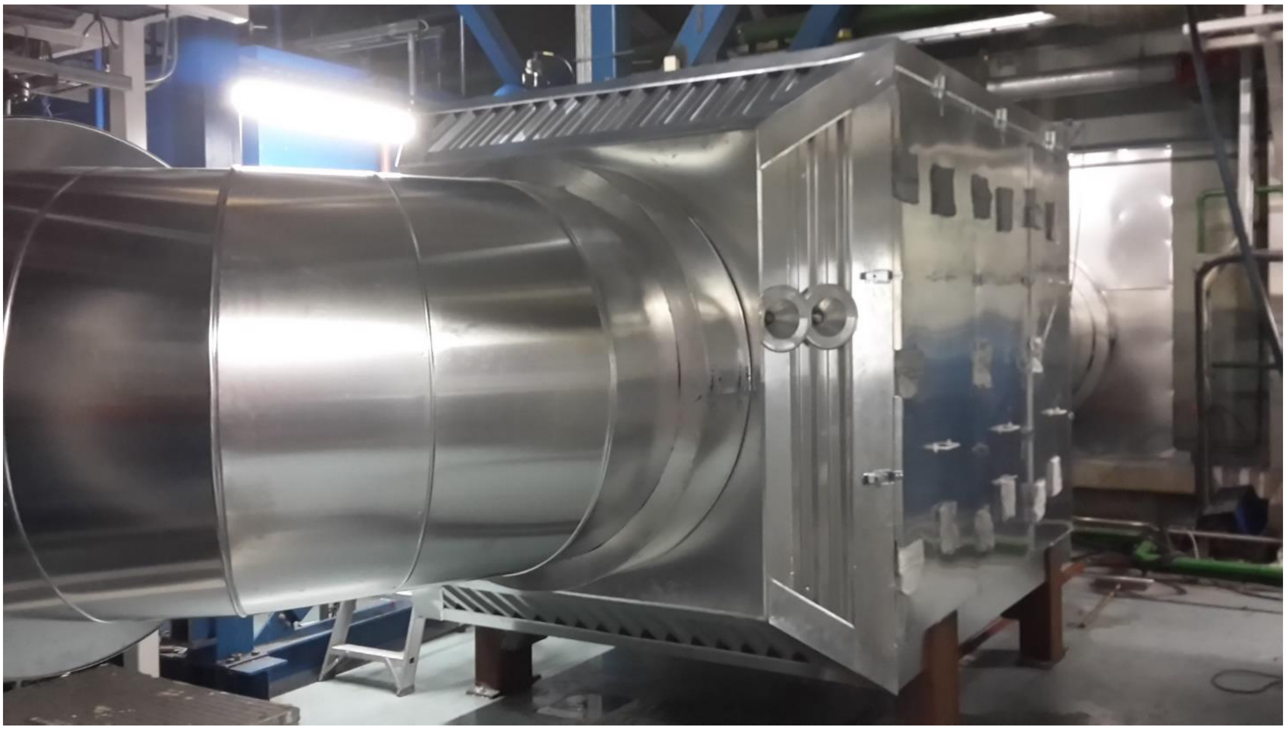

Figure 19: the SCR catalyst including “hotbox” insulation

Figure 20: control room during testing